SPIRE Bolometer Array Noise Performance during PFM 1, 2, and 3 Test Campaigns

Bernhard Schulz (IPAC)
with contributions from Jamie Bock, Hien Nguyen, Kevin Xu and Lijun Zhang

Contents

1. Introduction and scope

This note summarizes the noise performance of the PFM photometer and spectrometer detectors during the PFM1, PFM2 and PFM3 instrument tests respectively. The emphasis is on the derivation of the noise of the undisturbed detectors, hereafter called basic noise. We also make an assessment of the functionality of detector channels as far as measured, and discuss particular noise phenomena. Only one photometer dataset (2006-June-26) was taken with the photometer temperature control (PTC) active.

For the photometer, the data considered stems from the PFM2 and mainly from the PFM3 campaign. During the PFM2 campaign some LIA boards were missing, while during the PFM3 campaign the full complement was present. For the spectrometer we considered noise data from campaigns PFM1 and PFM3.

2. The data

Data was retrieved from databases PFM1_test2 and PFM3_test1 for the spectrometer arrays and PFM2_test1 and PFM3_test1 for the photometer arrays. Data that were analyzed for purposes of this document are listed in Table 1 below.

Generally the data were taken during the night with minimal optical loading, with the instrument on and the data acquisition system running. This way we expect a minimum of environmental disturbances. Although this was not always the case, our method to select the minimum noise provided reproducible results. The data from 12 and 13 June 2006 was discarded after discovering that light from the external window to the laboratory fell onto the detectors, creating random signal variations due to environmental changes and activities.

The data, especially from the first two test campaigns, are not very homogeneous. During PFM1 only the spectrometers were functional, during PFM2 a number of channels were not functional due to missing LIA boards, or due to an open connector, and during PFM3 the upper half of the SSW array was not

operational due to bias problems. Twelve more photometer pixels were not measured in PFM2 due to a JFET not turning on or broken lines.

Table 1: List of all test data considered for this analysis.

Date	Start	End	Campaign	Measurement Type
4-Mar-05	22:17	3:17	PFM1	Spectrometer Noise at different bias levels
9-Mar-05	0:22	10:07	PFM1	Spectrometer night noise
9-Mar-06	22:40	10:04	PFM1	Spectrometer night noise
24-Mar-05	10:55	12:46	PFM1	Spectrometer noise at different bias frequencies
29-Mar-05	9:34	9:37	PFM1	Spectrometer door slam test
8-Sep-05	22:12	4:42	PFM2	Photometer night noise
12-Sep-05	9:54	5:44	PFM2	Photometer night noise
14-Sep-05	23:16	10:47	PFM2	Photometer night noise
28-Sep-05	4:31	13:01	PFM2	Photometer night noise
8-May-06	19:05	21:16	PFM3	Photometer load curves
10-May-06	22:19	8:17	PFM3	Spectrometer noise
10-May-06	19:17	19:45	PFM3	Spectrometer load curves
12-May-06	21:38	6:39	PFM3	Photometer night noise
13-May-06	8:39	19:39	PFM3	Photometer noise
17-May-06	22:17	9:17	PFM3	Spectrometer noise
12-Jun-06	12:58	7:50	PFM3	Photometer noise
13-Jun-06	13:23	15:20	PFM3	Photometer noise
13-Jun-06	19:43	9:14	PFM3	Photometer noise
23-Jun-06	19:35	22:35	PFM3	Photometer noise
23-Jun-06	23:37	2:37	PFM3	Photometer noise
26-Jun-06	18:39	21:00	PFM3	Photometer PTC test

3. Processing

The data timelines were divided into 30 min intervals (9 min and 10 min pieces for the June 23 and June 26 data), and saved into FITS files. The signal and offset data were converted to volts, using the following formulae:

Photometer:
signal=5.*raw/((2^16-1)*12*454)
offset=5.*(52428.8*off-16384.0)/((2^16.-1.)*12*454)

Spectrometer:
signal=5.*raw/((2^16-1)*12*294)
offset=5.*(52428.8*off-16384.0)/((2^16.-1.)*12*294)

Signal and offset were then added. Each timeline interval was plotted as a signal timeline for visual inspection, and also transformed into a power spectrum. This transformation is done by first de-glitching the signal timeline using an iterative sigma kappa algorithm, then subdividing the timeline further into intervals corresponding to a lower limiting frequency of 0.01Hz. All intervals are Fourier transformed, normalized, and then quadratically added. This procedure yields a high S/N on the power spectrum.

The data time tags of the PFM1 and PFM2 campaigns contain errors that were automatically corrected. For the correction it was assumed that the majority of time tags are correct in absolute terms and that data are appearing in the correct order. Time tags were corrected such that the average data rate was kept. Two time errors were observed: one shows a sudden offset in time for a number of readouts, which reverts back after a while; the second shows short gaps of up to a few seconds duration, in an otherwise regular

sequence of data. For this analysis the first error was corrected by generating new time tags that are in sequence, the second error was corrected by shifting the entire remaining sequence back to remove the gap. For PFM3 data this problem has disappeared.

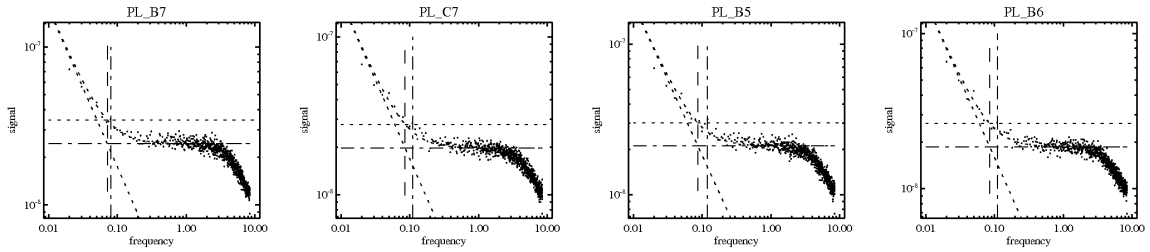

Figure 1 : Example power spectra derived from PLW data during PFM3 tests on 12 May 2006. The lines show white noise plateau levels and 1/f knee frequencies derived by two different methods. The signal is given in [V/sqrt(Hz)], the frequency is in [Hz].

4. Broken, noisy and peculiar channels

In the following the detector channels are designated by their QLA channel number in FULL mode, and by their JPL detector names. The prefixes PS, PM, PL, SS, SL identify the detector array.

The PFM1 tests with only the spectrometer detectors had all channels connected. However due to a harness problem, the shielding of a connector was compromised. The corresponding channel range 25-48 therefore exhibits excess noise, of which channels 25-42 are connected to detector pixels.

Due to the lack of some LIA boards during the PFM2 tests, the following photometer channel ranges were not available: 1-32, 129-160, 225-256. In addition the connector J31 of the photometer JFET module HSJFP was disconnected. These lines correspond to the PSW BDA connector J1, which corresponds to channels 49-72.

During the PFM3 test campaign the second spectrometer module (channels 25-48) failed to switch on. Due to the problems in the PFM1 tests, we have not analyzed any reliable data for these detector channels. We note however channels that were reported broken from assembly level testing at JPL.

In Table 2 we list a number of channels that were found to behave in a non-nominal way. Channels that deviate from the median noise by more than sqrt(2) are listed in column “Noisy”. Channels that exhibit noise levels of more than a factor of 2 more than the median are listed in column “Very Noisy”. The channels shown in column “Inop” were found to be not operational in the PFM3 test setup. For convenience the QLA channel number is given in brackets. The analysis was based on visual inspection of signal timelines and power spectra of noise measurements with constant operating parameters, as well as visual inspection of signal timelines of detector load curve data. The remarks following the channel number give possible reasons for failure or high noise:

- “short” means that a linear load curve like that of a resistor is observed.
- “BDA dead” means JPL test results indicate a broken bolometer.
- “nosig” means that the signal was outside the range of the A/D converter. A possible reason would be a broken line; however, the condition could also indicate problems with the offset circuit.
- “wrong polarity?” In several of the “nosig” cases the beginning of a load curve still shows a real signal that proceeds into the opposite direction than all other load curves.
- “loamp” means a load curve is seen, but with a much lower amplitude, suggesting the presence of strong attenuation of the signal along the line.

Photometer Arrays

Noisy	Very Noisy	Inop
PS_G13 (82) electronics	PS_C11 (23) low amp, electronics	PS_C12 (18) short, BDA dead
PS_DP2 (94) electronics	PS_B5 (54) unknown	PS_A10 (98) nosig, cryoharness
PS_B9 (106) electronics	PM_E4 (231) electronics	PS_J6 (123) loamp unknown
PS_F9 (134) electronics	PM_E5 (233) electronics	PS_G8 (132) short, BDA dead
PS_J10 (142) electronics	PM_F5 (235) electronics	PS_H9 (135) nosig, cryoharness
PM_B1 (270) electronics	PM_G6 (238) electronics	PM_C8 (215) nosig, unknown
PM_F6 (239) electronics	PL_A6 (148) Offset circuit	PM_T2 (219) nosig, cryoharness
PM_G7 (240) electronics	PL_C9 (150) electronics?	PM_F7 (252) nosig, wrong polarity?
PL_B1 (163) electronics		PM_G9 (257) loamp, unknown
		PM_B6 (276) nosig, wrong polarity?
PS_B12 (20) possibly noisy, electronics		PL_A2 (168) loamp, cryoharness
PM_A11 (201) possibly noisy, electronics		PTC3 (288) nosig wrong polarity
PM_C1 (273) perhaps noisy		

Problematic Channels	
PS_A13 (12) long time constant (360 ms)	PS_J7 (128) intermittent
PS_A11 (22) long time constant	PS_G11 (144) possibly intermittent
PS_D11 (97) long time constant (45.4 ms)	PM_A13 (193) long time constant
PS_A10 (98) long time constant (41.4 ms)	

Spectrometer Arrays

Noisy	Very Noisy	Inop
SS_A3 (3)	SS_A2 (4)	SS_D5 (29) broken in BoDAC
SS_E3 (16)	SL_E2 (60)	SL_C2 (57) nosig
SL_C1 (51)		SL_B3 (64) nosig
SL_D2 (58)		SL_DK2 (67) broken in BoDAC
SL_A3 (71)		
SL_T2 (72)		
SS_F4 (41) noisy in BoDAC		
	electronics: could be JFET or LIA because pixel noise > 20nV/sqrt(Hz) when measured at 2K	*short=short between detector contacts* *nosig=no signal* *loamp=low amplification*

Table 2: Listing of noisy, very noisy and non-operational detector channels in the photometer arrays. See text for a definition of terms.

It should be noted that channels, PS_F14(83), PS_H16(93) and PS_E9(104) were not measured in BoDAC, but are nevertheless functional on instrument level. There is a possibility that PS_G11(144) is intermittent, as it showed strong noise in the early PFM3 tests but was fine later. From a PCAL measurement performed June 21, 2006 11:39, we found two more pixels with long optical time constants. These are PS_A11(22) and PM_A13(193), which are listed as problematic in Table 2. The following channels were found to have no or little optical response. These were PS_A13(12) with low optical response, PS_D12(19) being noisy but with large signal, and PS_B5(54) which appears optically dead. The channel PM_C1(273) showed no signal in this particular test, probably due to a bad offset circuit. Otherwise it is seen as a perhaps noisy pixel. These pixels will need additional insvestigation.

For the spectrometer our knowledge is more limited due to the repeated problems with the channel range 25-48, encompassing the second JFET module of the SSW array. There are 4 known broken channels, 2 that are very noisy, and 6 that fall under the noisy criterion. The list of pixels is given in Table 2. Within the range of the un-tested second module of the SSW, the SS_F4(41) channel is known to be noisy from BoDAC tests, and channel SS_D6(28) was not measured in BoDAC but shows reasonable noise levels in the PFM1 tests. The channels SS_DK1, SS_B3, SS_D3, SS_D1, SS_E1 were found noisy in BoDAC, but seem not to be peculiar in the instrument tests.

5. Basic noise

To measure the white noise level, the power spectra for each pixel and each individual 30 min (9,10 min) dataset were calculated. From the power spectrum (see Fig. 1) the white noise level is determined as the median of the 0.5-3.0 Hz interval. As any external disturbance of the system will make the noise level increase, it is safe to derive the basic noise level for a given pixel as the smallest noise value derived over all timeline subdivisions.

The minimum noise levels for one bias level and frequency is shown in Figs. 2-6. The four diagrams are showing measured noise values and model prediction for each channel, a histogram of differences between data and model, the measured 1/f knee frequency for each channel, and a histogram of all 1/f knee frequencies.

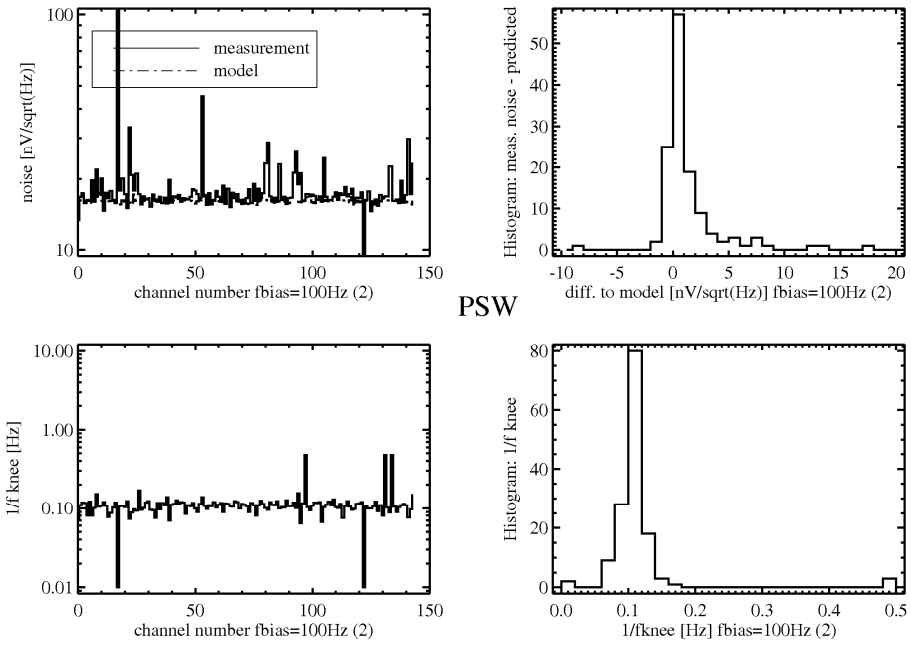

Figure 2: Starting top left, the figures are showing a) measured noise vs. channel number and model prediction, b) histogram of differences between data and model, c) 1/f knee frequency vs. channel number and d) histogram of 1/f knee frequencies for the PSW arrays.

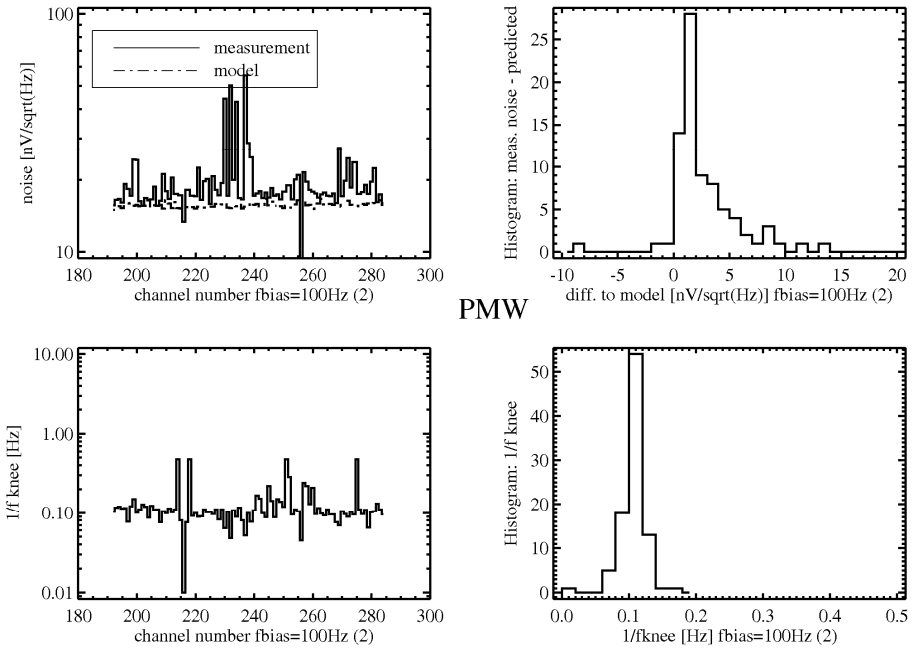

Figure 3: Same as previous figure but for PMW array.

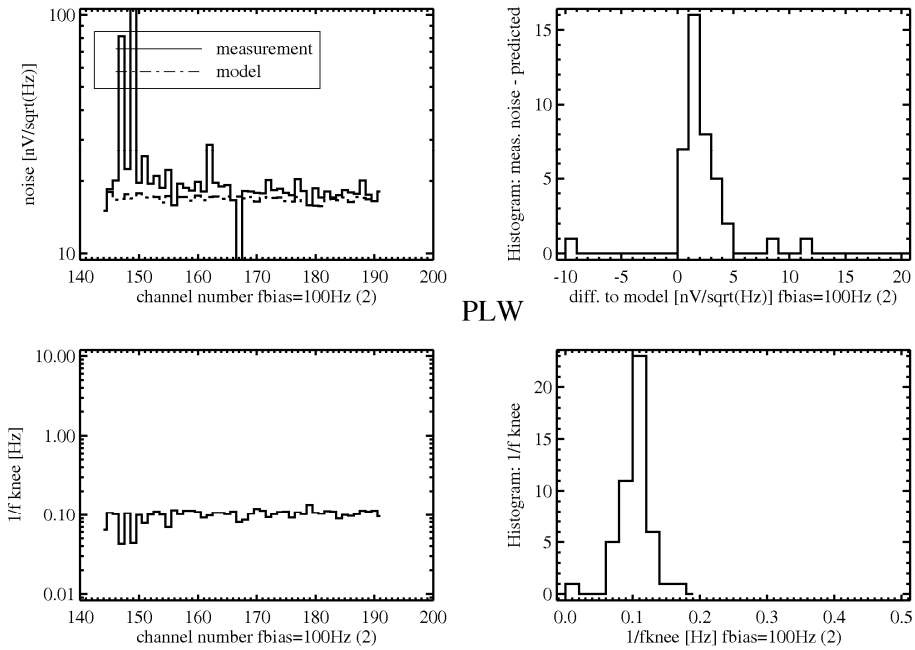

Figure 4: Same as previous figure but for PLW array.

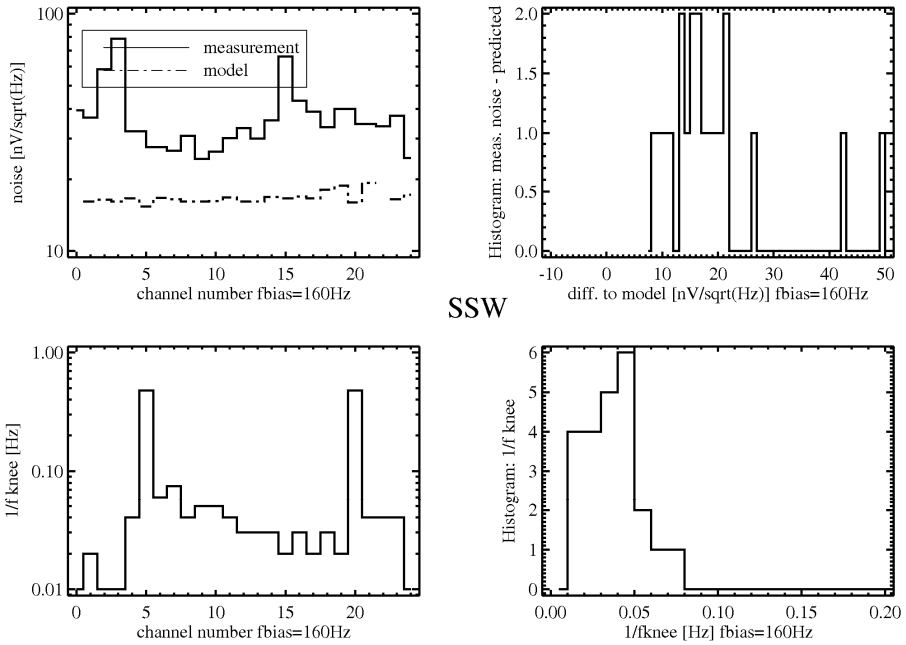

Figure 5: Same as previous figure but for SSW array.

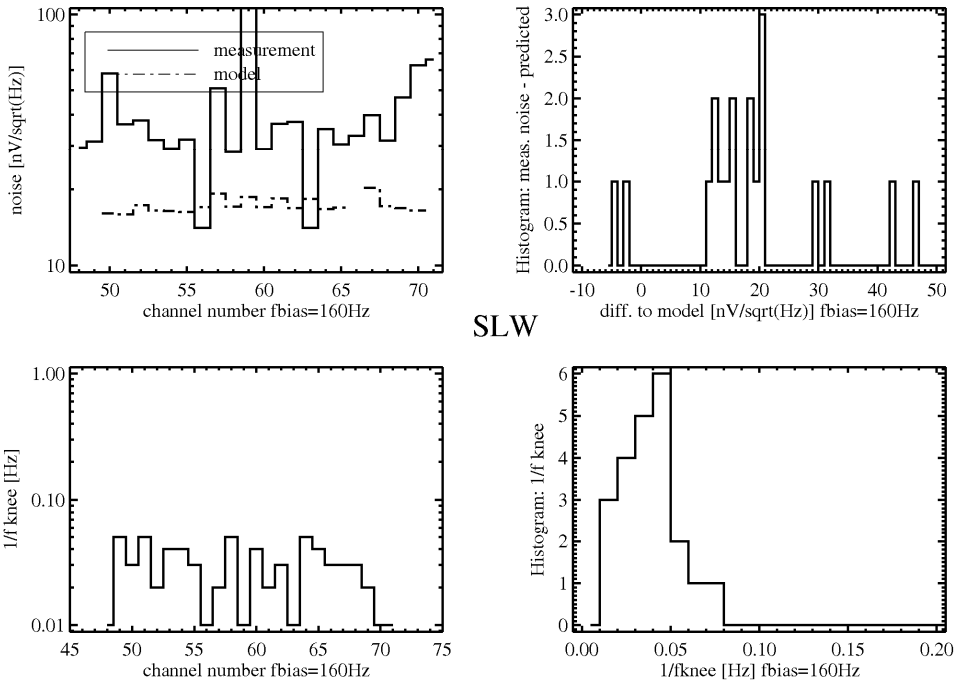

Figure 6: Same as previous figure but for SLW array.

Expected noise levels were derived from standard bolometer theory according to Mather, using the JPL measured characteristic bolometer parameters, and actual temperatures. We assumed zero optical power on the detectors, which is not entirely correct for the PLW and SLW. We also assumed 10 nV/sqrt(Hz)

amplifier noise, which turned out to be too low for the spectrometer channels of this version of the warm electronics. The modelled noise appears in Figs. 2-6 as dash-dotted line. For the SSW we show only the lower 24 channels since the upper half of channels didn't switch on due to biasing problems with the JFET module.

The measured values for the photometer agree quite nicely with the predictions as seen in Figs. 2-4. One JFET module that corresponds to channels 241 to 264 (BDA connector J02) was under-biased. These channels show erratic signal timelines as illustrated in Fig. 7.

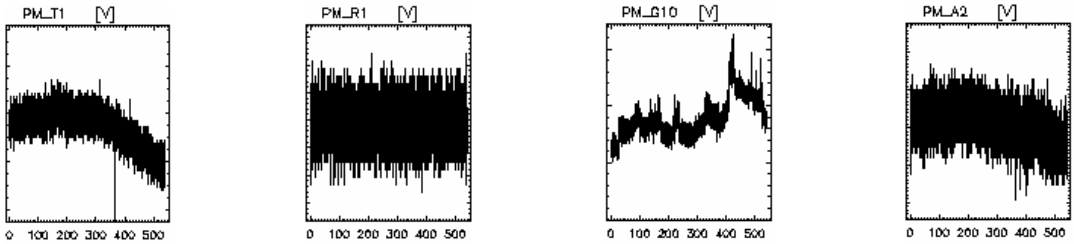

Figure 7 : Contemporaneous signal timelines of a thermistor pixel, a resistor pixel, and pixels G10 and A2 of the PMW array. The x-axis is scaled in seconds. Major tickmarks on the y-axis are 200 nV, 100 nV, 500 nV, and 100 nV, on the diagrams for PM_T1, PM_R1, PM_G10, and PM_A2 respectively. The G10 pixel is an example of erratic behaviour due to under-biasing of a JFET module.

The spectrometer channels exhibit considerably larger noise than predicted (see Figs. 5 and 6). These values were corrected to higher values by a factor 454/294, compared to a previous version of this report, after an error in the signal conversion was discovered. The cause for the rather large noise figures is under investigation, as the noise is also larger than the BoDAC measurements indicate. The amplifier noise of the warm electronics being used currently is known to be higher than specified. To make the model more consistent with the data requires an increase of the amplifier noise to 22 nV/sqrt(Hz). A measurement of the amplifier noise with warm JFETs gave a similar result, yielding 20 nV/sqrt(Hz) (e-mail: B. Swinyard 13 Sept 2006).

The median of all measured noise values of a bolometer array can be considered a representative value. To give an overview over noise performance under different operating conditions, as analyzed of the 3 instrument test campaigns, we have plotted the median noise values per array versus either bias level or bias frequency, distinguishing the respective other dimension with different symbols and line styles (see Figs. 8-10). The horizontal lines show the model predictions corresponding to the measurements.

6. 1/f Noise and temperature instabilities

The lower two diagrams in Figs 2-6 show the lowest achieved 1/f noise per pixel during a series of measurements conducted on 10 May 2006 (spectrometer) and 23 June 2006 (photometer). The left diagram gives the noise per pixel and the right diagram shows a corresponding histogram. The photometer arrays peak at about 100 mHz, while the spectrometer arrays show a much lower peak 1/f knee frequency of 40 mHz.

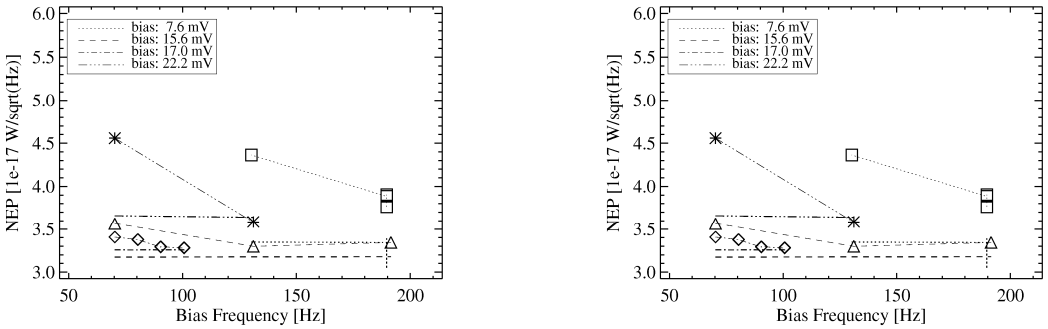

Figure 8: Measured median noise levels for the PSW (left) and PMW (right) at different biases and bias frequencies. The horizontal lines show the model predictions under the respective conditions. The measurement series at 17.0 mV bias is the only one showing a reproducible trend with bias frequency.

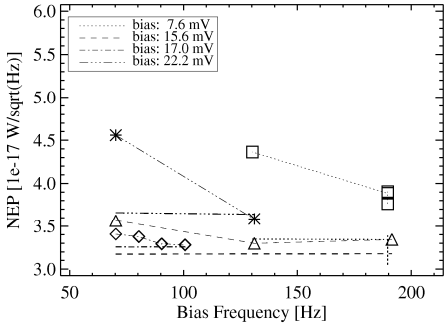

Figure 9: Measured median noise levels for the PLW at different biases and bias frequencies. The horizontal lines show the model predictions under the respective conditions.

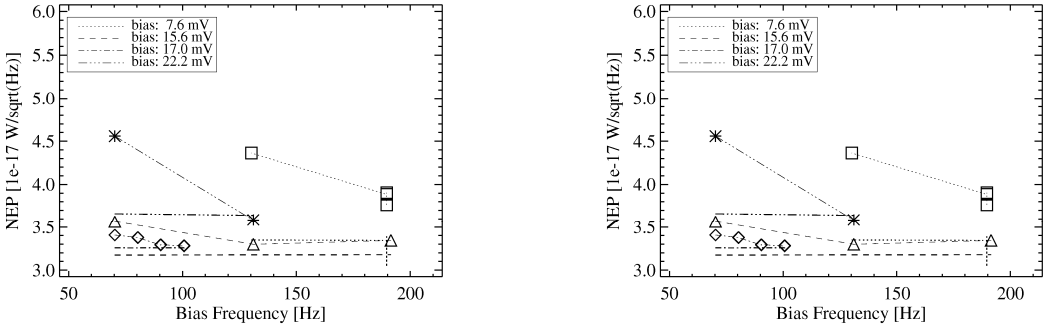

Figure 10: Measured median noise levels for the SSW (left) and SLW (right) at different biases and bias frequencies. The horizontal lines show the model predictions under the respective conditions.

These values are, however, dominated by temperature drifts of the cryostat and the ^{3}He fridge. On first sight the values for the spectrometer seem to correspond well to those reported by unit level measurements. However, since 1/f knee frequency and white noise plateau are not independent of each other, the almost by a factor 2 higher noise values than predicted, may just mask some of the long-term variations and thus lower the measured 1/f knee.

Figure 11: Plots of ant correlated drifting signals of bolometer detector PS_H5 and the 300mK temperature sensor.

Insufficient temperature stability of the bolometer base plate is the main reason for an increased 1/f knee in the instrument level tests. This conclusion is drawn from the observation that all functional bolometer signals follow the same drift pattern, while the resistor signal remains stable. Additionally the temperature sensor connected to the cold finger (SUBKTEMP) shows a strong anti-correlation with the signal of the functional bolometers including the available thermistor pixels, although the resolution of its A/D converter is rather limited (see Fig. 11). We further verified with simulated detector data that a slope in the signal timeline raises the 1/f knee frequency but does not impact the white noise level as long as both components can be distinguished in the power spectrum.

Deriving the detector bath temperature from the thermistor pixels T2 of each photometer array, we used the Mather detector model to convert the detector signal into optical in-band power. The median array values taken over the minimum noise values for each pixel are shown in Fig. 12. The left diagram was derived from the uncorrected signal timeline, the right one was derived from the timeline of optical powers. The median values are plotted against bias frequency, which was the variable parameter during the measurement sequence conducted on 23 June 2006. The right diagram shows a general improvement of the 1/f knee values. It remains to be verified whether errors in the model parameters are preventing a stronger improvement. It may be possible that a simple empirical correction, based on the correlation of thermistor signal and detector signals, works even better.

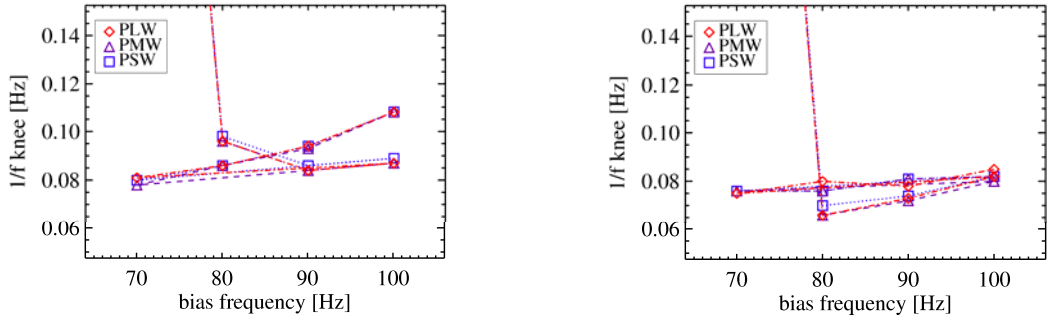

Figure 12: The diagrams show the median array 1/f knee values for the measurements of 23 June 2006 before (left), and after (right), removal of the temperature drifts using the bolometer model.

7. Noise during PTC tests

A set of photometer noise measurements, where the PTC was operated in closed loop, has been reduced in the same way as the other noise measurements. The results are plotted in Figs. 13 – 15.

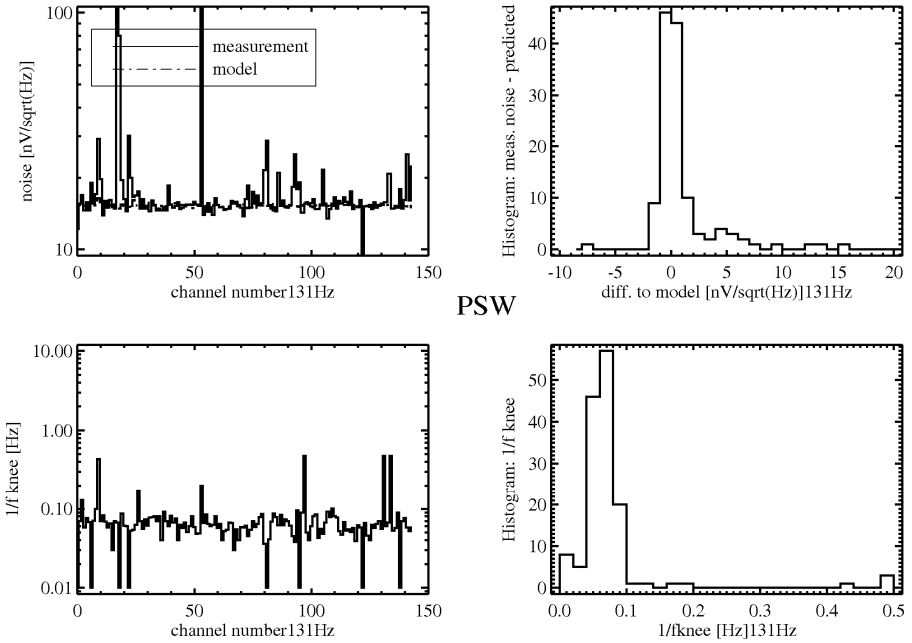

Figure 13: The diagrams show the median array 1/f knee values for the measurements of 23 June 2006 before and after removal of the temperature drifts using the bolometer model.

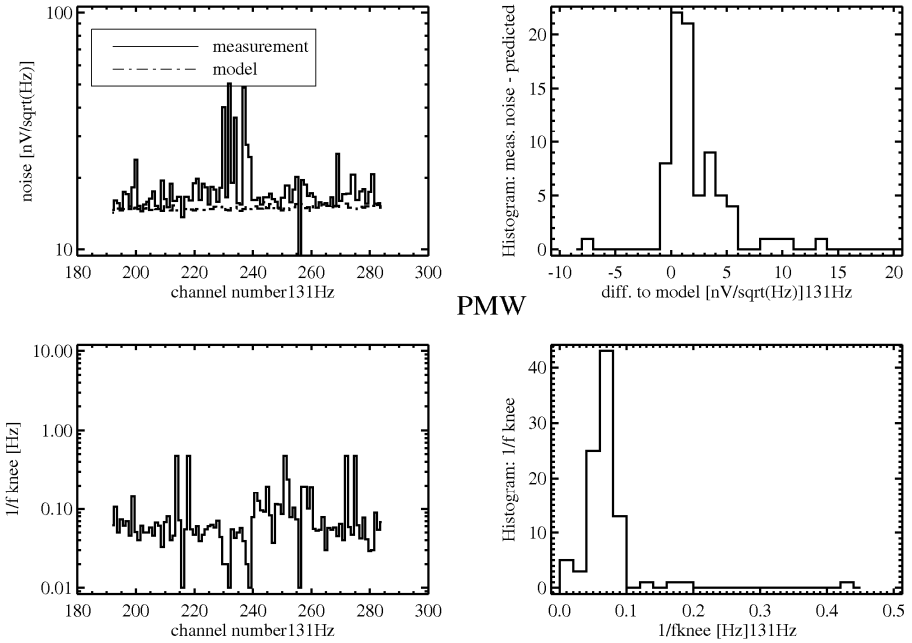

Figure 14: The diagrams show the median array 1/f knee values for the measurements of 23 June 2006 before and after removal of the temperature drifts using the bolometer model.

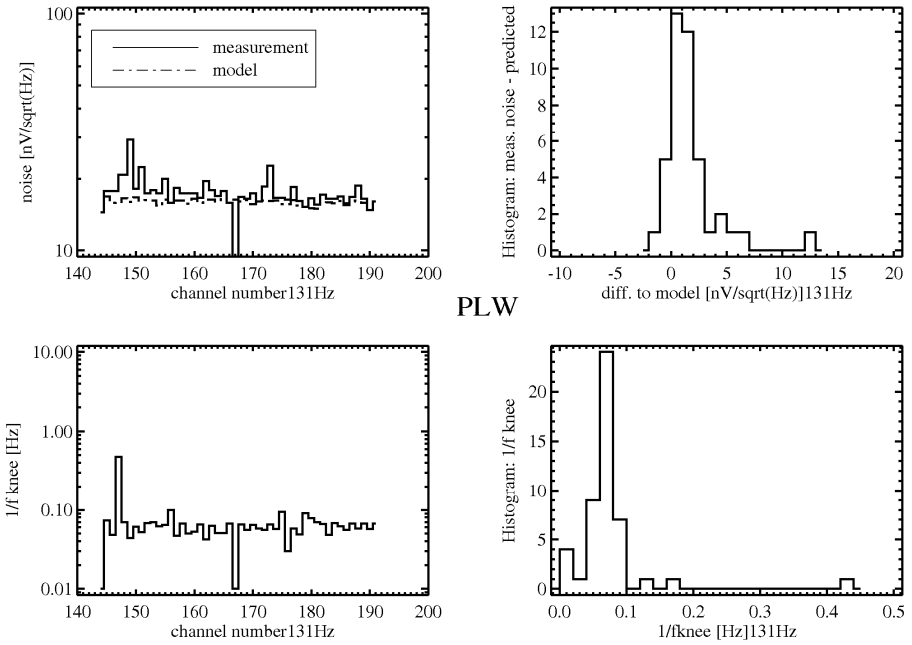

Figure 15: The diagrams show the median array 1/f knee values for the measurements of 23 June 2006 before and after removal of the temperature drifts using the bolometer model.

Comparison of these figures with Figs. 2-4 shows an improved 1/f knee frequency while temperature control is on. During the noise measurements without PT control, the distribution of 1/f knee frequencies is centred around 100 mHz, whereas with an active PTC the distribution shifts down by 30 to 40 mHz. Fig. 15 seems even to suggest an improvement in the white noise for the PLW, but that may also be an effect of the different bias frequency.

While the PTC is on, the power spectra don't show any unusual features, except a very strong 800 mHz line in the thermistor channels PTC1 and 2 as illustrated in Fig. 16. No noise disturbances or spectral features are recognizably coming from the PTC operation.

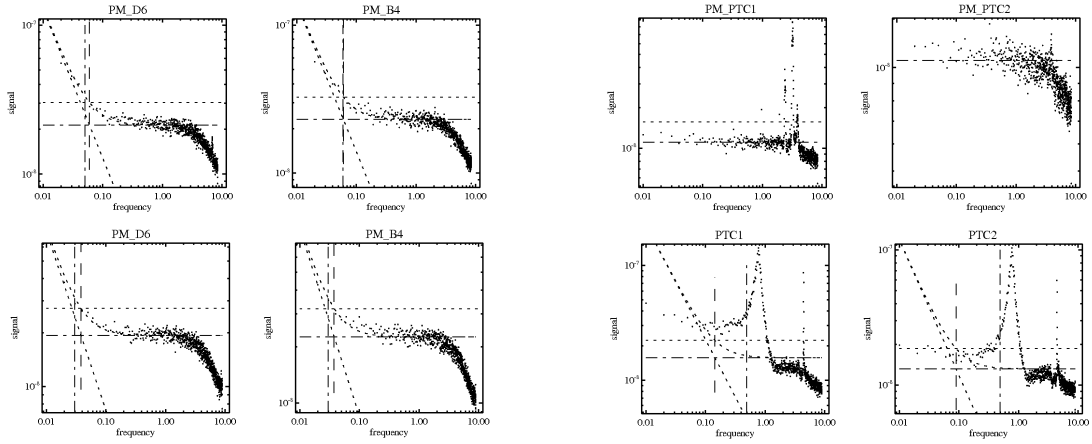

Figure 16: Example power spectra of detector signals (left) and the PTC thermistor signals (right) with the PTC off (top row: 12 May 06) and the PTC operating in closed loop (bottom row: 26 June 06). Note in the bottom row the low 1/f knee of the detector signals (left) and the strong 800 mHz line that results from the control feedback. The y-axis is in Volts and the x-axis in Hz.

The modulated punch-through is shown in Fig. 17, which was measured from periodic switching of the PTC heater with varying power settings and at different switch frequencies.

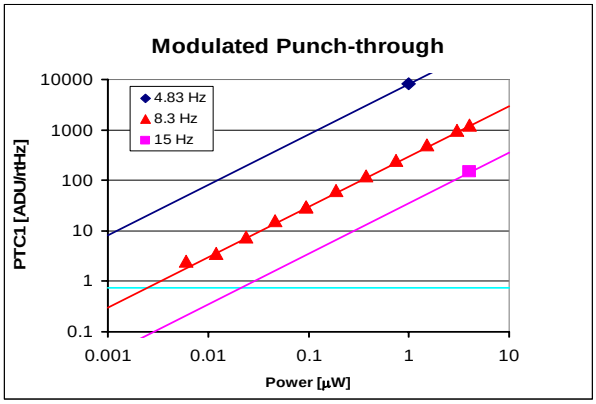

Figure 17: This diagram shows the amount of detected noise power in the thermistors PTC1 and 2, while the thermal control was switched repeatedly with the power difference given on the x-axis and the noise on the y-axis given in ADU/sqrt(Hz).

8. Spectral features

High S/N co-added power spectra of several hours display a number of features that sometimes vary from one night to the other. Among others, we found in PSW pixels a broad 5-Hz bump, which appears sometimes also as sharper microphonic line. The PLW array sometimes exhibits a bump centred at 1 Hz. The PMW shows several broad features somewhat similar to the 1Hz feature of the PLW. Most PMW channels also show a sharp 7-Hz line. The overall picture of these features looks rather inconclusive, as they vary from one measurement series to the next, and may be driven by external influences of the test site at RAL.

9. Spontaneous spiking

During the PFM2 campaign we observed at times instantaneous spontaneous spiking of the signal in the PSW signals (See Fig. 18). This was correlated in all functional detector pixels of this array. The PLW and PMW arrays showed some obviously related baseline drift, but only few spikes during the same time. Different types of spikes are observed as illustrated in Fig. 19, showing signals from exemplary pixels of the PSW, PLW and, PMW arrays and an overplotted smoothed baseline signal (in gray), that most other pixels of the respective detector array are following. All three arrays show a strong thermal spike with a large time constant. In addition the PSW and the PMW show one and two additional spikes respectively with a shorter time constant, which is not seen in the other arrays. It appears that at least some of this behaviour is due to too non-optimal bias selections for the JFET arrays, which was particularly prominent in module 11 (channels 241-264).

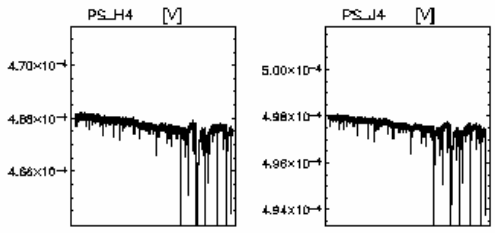

Figure 18: Spontaneous spiking occurring within a 30 min interval.

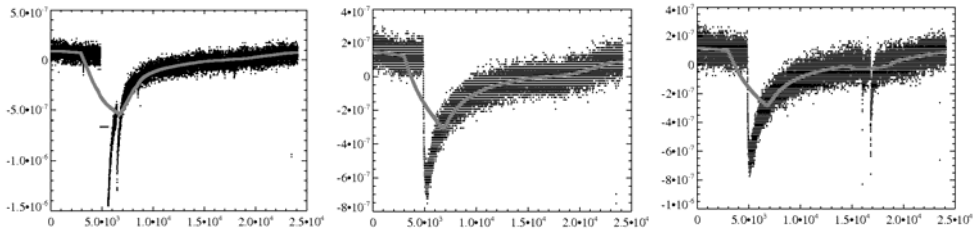

Figure 19: Contemporal signal plots versus time of exemplary detector pixels of PSW, PLW and PMW detectors (from left to right). Different spike types can be seen.

10. Influence of bias frequency

As verified in the PFM1 spectrometer tests, and PFM3 photometer tests, the bias frequency also has an important influence on the noise. Fig. 20 shows the median noise (excluding the noisy second module of SSW) over the spectrometer arrays depending on bias frequency. The lowest noise is found for 106-Hz bias frequency, while encountering a particularly high noise level at 70 Hz.

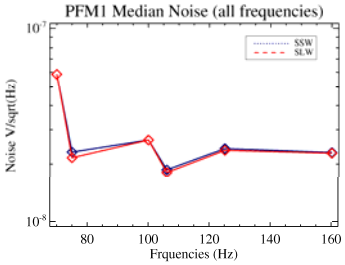

Figure 20: Median array noise depending on bias frequency for the spectrometer arrays (note: The plotted values need to be multiplied by a factor 1.62).

Figure 21: Median array noise depending on bias frequency for the photometer arrays. The left diagram shows the measured noise, the right diagram shows the NEP after removing temperature drifts with the Mather bolometer model.

A summary of all measurements with different bias frequencies is shown in Figs. 8-10, however the scatter among measurements is fairly high, and other external influences seem to have a large influence on the results. A fairly reproducible dependency of noise on bias frequency for the photometer detectors could be found in the June 23 measurements as (see Fig. 21). It is also interesting to note that the consistency of the data points improves after treatment with the bolometer model, implying responsibility of temperature drifts for the differences in the left diagram.

11. Summary and conclusions

1. Data from all five SPIRE PFM detector arrays were analyzed regarding detector noise. Data time tags had to be corrected during the PFM1 and PFM2 campaigns. The inhomogeneity of the dataset leaves the spectrometer channels 25-42 yet insufficiently characterized on instrument level.

2. For the photometer, 12 channels and in the spectrometer at least 4 channels were found not to be operational in PFM3 tests. In the photometer, 9 channels were found to be “noisy”, and 8 channels were found to be “very noisy”, generally due to electronics issues. In the spectrometer 7 “noisy” and 2 “very noisy” pixels were identified. 7 more pixels in the photometer suffer from having long time constants or being intermittent. Including “very noisy” pixels and pixels with long time constants as non-operational, we find 11, 10, 3, 2, and 4 channels for PSW, PMW, PLW, SSW, and SLW, respectively that were not operational in PFM3. Four more PSW channels were found not to react to optical signal changes, invoked by the BSM. This will, however, require more investigation.

3. The large majority of photometer signals show only 10-20% more noise respectively than theoretical expectations from model calculations made for the actual biases and temperatures that were used. The spectrometer channels show about a factor of 2 more noise than expected, mainly due to increased warm electronics noise, which is still being investigated. The basic spectrometer noise seems also to exhibit a stronger dependence on bias frequency.

4. The quiet signal is disturbed by variations and instability of the base plate temperature, which were stronger and more erratic for the PFM2 tests. In addition strong spikes were observed, that sometimes appear in series. They show at least two different time constants, and can appear solely on one detector array, or on all three photometer arrays simultaneously. The PFM3 tests showed less of these events.

5. The surprisingly large noise levels found in the spectrometer need to be investigated. Since the detectors on average showed low noise values in BoDAC, the most likely source is either the warm electronics or badly biased JFETs. There is still the chance that these problems are solved with the replacement of the warm electronics by the PFM model.

6. The basic white noise levels found for the photometer look satisfactory, and are quite close to the theoretical expectations. The 1/f knee frequencies are generally within the requirement of <100mHz and could be lowered further in the analysis by removing temperature related drifts using the thermistor pixels and/or operating the PTC.

7. Operating the PTC in closed loop works according to expectations and lowers the 1/f knee frequencies down to 60-70 mHz, similar to the software method.

8. For future testing, particular care should be taken to set the correct JFET bias levels, as well as to ensure that external influences including variable straylight from the outside of the cryostat are kept to a minimum. It seems now that much of the unexplained signal variation and spiking, observed during the PFM2 and PFM3 campaigns, were due to incorrectly biased JFETs, straylight, and microphonics from the lab.